BRAIN
A JOURNAL OF NEUROLOGY

The structural plasticity of white matter networks following anterior temporal lobe resection

Mahinda Yogarajah,[1] Niels K. Focke,[2] Silvia B. Bonelli,[1] Pamela Thompson,[1] Christian Vollmar,[1] Andrew W. McEvoy,[3] Daniel C. Alexander,[4] Mark R. Symms,[1] Matthias J. Koepp[1] and John S. Duncan[1]

1 Department of Clinical and Experimental Epilepsy, UCL Institute of Neurology, and National Society for Epilepsy, London, WC1N 3BG, UK
2 Department of Clinical Neurophysiology, University of Goettingen, 37099 Goettingen, Germany
3 Department of Neurosurgery, National Hospital for Neurology and Neurosurgery, UCLH, London, WC1N 3BG, UK
4 Department of Computer Science, UCL, London, WC1E 6BT, UK

Correspondence to: Prof. John S. Duncan,
Department of Experimental and Clinical Epilepsy,
UCL Institute of Neurology,
Queen Square London,
WC1N 3BG UK
E-mail: j.duncan@ion.ucl.ac.uk

Anterior temporal lobe resection is an effective treatment for refractory temporal lobe epilepsy. The structural consequences of such surgery in the white matter, and how these relate to language function after surgery remain unknown. We carried out a longitudinal study with diffusion tensor imaging in 26 left and 20 right temporal lobe epilepsy patients before and a mean of 4.5 months after anterior temporal lobe resection. The whole-brain analysis technique tract-based spatial statistics was used to compare pre- and postoperative data in the left and right temporal lobe epilepsy groups separately. We observed widespread, significant, mean 7%, decreases in fractional anisotropy in white matter networks connected to the area of resection, following both left and right temporal lobe resections. However, we also observed a widespread, mean 8%, increase in fractional anisotropy after left anterior temporal lobe resection in the ipsilateral external capsule and posterior limb of the internal capsule, and corona radiata. These findings were confirmed on analysis of the native clusters and hand drawn regions of interest. Postoperative tractography seeded from this area suggests that this cluster is part of the ventro-medial language network. The mean pre- and postoperative fractional anisotropy and parallel diffusivity in this cluster were significantly correlated with postoperative verbal fluency and naming test scores. In addition, the percentage change in parallel diffusivity in this cluster was correlated with the percentage change in verbal fluency after anterior temporal lobe resection, such that the bigger the increase in parallel diffusivity, the smaller the fall in language proficiency after surgery. We suggest that the findings of increased fractional anisotropy in this ventro-medial language network represent structural reorganization in response to the anterior temporal lobe resection, which may damage the more susceptible dorso-lateral language pathway. These findings have important implications for our understanding of brain injury and rehabilitation, and may also prove useful in the prediction and minimization of postoperative language deficits.

Introduction

Temporal lobe epilepsy (TLE) is the most common cause of medically intractable partial epilepsy in adults (Engel, 1998). In ~40% of patients with TLE, seizures continue despite trials with three or more antiepileptic drugs (Semah et al., 1998). For this group of patients, anterior temporal lobe resection is now a well-established and effective means of treatment (Wiebe et al., 2001). Though up to 80% of these patients may be rendered seizure free by surgery, up to 40% are also at risk of postoperative decline in memory and language functioning (Wiebe et al., 2001). Several functional magnetic resonance imaging (fMRI) and magnetoencephalography (MEG) studies have attempted to elucidate the functional reorganization that occurs after surgery (Backes et al., 2005; Noppeney et al., 2005; Pataraia et al., 2005; Maccotta et al., 2007; Cheung et al., 2009; Wong et al., 2009). Few studies have assessed the structural consequences of epilepsy surgery (Concha et al., 2006, 2007; Schoene-Bake et al., 2009; Yasuda et al., 2009). Moreover, none of these studies have longitudinally assessed the nature of white matter changes after neurosurgery, and how these changes relate to functional and neuropsychological outcome in patients.

Diffusion tensor imaging (DTI) is an advanced MRI technique, which measures the magnitude and direction of diffusion of water molecules within each voxel in an image (Basser, 1995). It can be used to probe the microstructure of white matter tracts, and provides the basis for non-invasive diffusion tensor tractography that can be used to map white matter pathways (Mori and van Zijl, 2002). The non-invasive *in vivo* nature of this technique allows for the longitudinal evaluation of white matter tracts in individuals. Whole-brain voxel-wise analysis of data obviates the need for restriction to *a priori* regions, which can bias the interpretation of such data, and provides morphometric information regarding the changes that may occur in white matter after neurosurgery. There are several voxel-based methods that can be applied; tract-based spatial statistics (TBSS) encompasses high sensitivity to, and excellent interpretation of, white matter tract changes in patients with temporal lobe epilepsy (Focke et al., 2008). This method uses a nonlinear form of registration specifically optimized for diffusion data, and projects data from individual patients onto an alignment invariant, group tract representation. This precludes the need for spatial smoothing of data, which can hinder the sensitivity and interpretation of the results (Jones et al., 2005; Smith et al., 2006). Significant clusters identified at a group level by such methods can then be deprojected and back normalized into individual subjects in order to provide quantitative information in each subject that can be statistically analysed. These regions can also be used as seed regions for tractography that provides complementary information regarding the morphology of those areas identified with voxel-based methods.

We applied these techniques to a group of patients with TLE in whom DTI data was acquired before and after anterior temporal lobe resection. The aims of this study were, first, to assess on a voxel-wise basis, and without any *a priori* hypothesis, the location and extent of structural white matter changes after temporal lobe surgery. Second, to investigate the causes of these changes and how they relate to expressive language function outcome in these patients.

Methods

Subjects

We studied 26 left (mean 37 years, range 18–62 years, 10 male) and 20 right (mean 37 years, range 22–52 years, 8 male) TLE patients, all of whom were medically refractory. All patients underwent pre-surgical evaluation, and subsequent anterior temporal lobe resection for the treatment of their epilepsy, at National Hospital for Neurology and Neurosurgery, London, UK. All patients had undergone structural MRI at 3 Tesla (3T) (Duncan, 1997), and video EEG had confirmed seizure onset in the temporal lobe ipsilateral to the resection. Six out of 26 left and two of 20 right TLE patients also had intracranial recordings to localize seizure onset to the temporal lobe ipsilateral to the resection. Four of the 26 patients with left TLE had normal structural MRI, and histopathology of the resected specimen revealed end folium sclerosis. Two of the 20 right TLE patients had anterior temporal lobe cavernomas and one had a normal structural MRI, and histopathology of the resected specimen revealed end folium gliosis. All remaining patients had hippocampal sclerosis identified on MRI ipsilateral to seizure onset, and all patients had a normal, contralateral hippocampus based on qualitative and quantitative MRI (Woermann et al., 1998). Postoperative histopathology confirmed the MRI findings in all cases. All patients were taking anti-epileptic medication and all, except two patients with TLE, spoke English as a first language. Handedness was determined using the Edinburgh handedness inventory (Oldfield, 1971), and language dominance was determined using a range of fMRI tasks, which have been described previously, and include the use of verbal fluency measures (Powell et al., 2006). In brief, this paradigm consisted of a blocked experimental design with 30-s activation blocks alternating with 30 s of cross-hair fixation during the baseline condition over 5.5 min. During the activation phase, subjects were asked to covertly generate different words beginning with a visually presented letter (A, S, W, D and E). The data were analysed using statistical parametric mapping (SPM5) [Wellcome Trust Centre for Imaging Neuroscience (http://www.fil.ion.ucl.ac.uk/spm/)]. Scans from each subject were re-aligned using the mean image as a reference, spatially normalized into standard space (using a scanner-specific template created from 30 healthy controls, 15 patients with left hippocampal sclerosis and 15 patients with right hippocampal sclerosis) and spatially smoothed with a Gaussian kernel of 10 mm FWHM. Lateralization indices were derived in subjects using the bootstrap method of the SPM lateralization index toolbox (Wilke and Lidzba, 2007), which was applied to the verbal fluency contrast in the middle and inferior frontal gyri. Patients with a laterality index of less than −0.4 or more than 0.4 were described as left and right dominant, respectively, while those patients with laterality indices between −0.4 and 0.4 were described as having bilateral representation of language (Briellmann et al., 2003).

The standard neurosurgical procedure undergone by these patients consisted of the removal of the temporal pole, opening of the temporal horn, followed by en bloc resection of the hippocampus with a posterior resection margin at the mid-brainstem level. Typically, the anterior–posterior extent of the temporal lobe resection as measured from the temporal pole to the posterior margin of resection is 30% and 35% of the distance from the temporal pole to the occipital pole after left and right anterior temporal lobe resection, respectively.

The study was approved by the National Hospital for Neurology and Neurosurgery and the Institute of Neurology Research Ethics Committee, and informed written consent was obtained from all patients. Patient demographics, clinical information and surgical outcome data [based on the ILAE classification of postoperative seizure outcome (Wieser *et al.*, 2001)] at the time of the postoperative scan following epilepsy surgery are listed in Table 1.

Neuropsychology

All patients, except the two in whom English was not their first language, completed the McKenna Graded Naming Test pre- and postoperatively. In this test, the subject is asked to name 30 black and white line drawings of increasing difficulty. The total number of items correctly named is the performance indicator (McKenna and Warrington, 1983). The same patients also performed two verbal fluency tests pre- and postoperatively. In the first-letter fluency test, the patient is given 60 s to produce as many words starting with the letter 'S', and in the second category fluency test, the subject is asked to name as many animals as possible. The total number of words correctly produced is the performance indicator (Spreen and Strauss, 1998). Using these raw values, the percentage change following surgery of each parameter was calculated using the following formula:

$$\left[\frac{\text{post operative value} - \text{preoperative value}}{\text{preoperative value}}\right] \times 100$$

We expected a high degree of correlation between the letters 'S' and 'A' in the preoperative scores, postoperative scores and percentage changes in verbal fluency. Therefore, we used a principal components analysis within SPSS v14.0 (SPSS Inc. Chicago, IL, USA) to identify a factor accounting for the largest component of variance amongst each of these three pairs of scores. For all three pairs, both measures were entered into a principal components analysis, from which the first principal component was extracted and used to represent overall pre- and postoperative verbal fluency and change in verbal fluency following surgery.

MR data acquisition

MRI studies were performed on a 3 T GE Excite II scanner (General Electric, Wakashua, Milwaukee, WI, USA). Standard imaging gradients with a maximum strength of $40\,\text{mT m}^{-1}$ and slew rate $150\,\text{T m}^{-1}\text{s}^{-1}$ were used. All data were acquired using a body coil for transmission, and 8-channel phased array coil for reception. The scanning protocol also included a coronal T_1-weighted volumetric acquisition sequence with 1.1-mm thick slices, and hippocampal volumes were determined using a previously described method (Moran *et al.*, 1999). A single investigator (M.Y.) manually segmented the surgical resection area of each patient's postoperative T_1-weighted volumetric MR scan, creating individual regions of interest (ROI). These ROIs were used to quantify the volume of resection in each patient.

Diffusion tensor image acquisition

The DTI acquisition sequence was a single-shot spin-echo planar imaging (EPI) sequence, cardiac gated with TE = 73 ms. Sets of 60 contiguous 2.4-mm thick axial slices were obtained, covering the whole brain, with diffusion-sensitizing gradients applied in each of 52 non-collinear directions [maximum b value of $1200\,\text{mm}^2\,\text{s}^{-1}$ ($\delta = 21\,\text{ms}, \Delta = 29\,\text{ms}$, using full gradient strength of $40\,\text{mT m}^{-1}$)] along with six non-diffusion-weighted ($b=0$) scans. The gradient directions were calculated and ordered as described elsewhere (Cook *et al.*, 2007). The parallel imaging factor (SENSE) was 2. The field of view was 24 cm, and the acquisition matrix size was 96×96, zero filled to 128×128 during reconstruction so that the reconstructed voxel size was $1.875 \times 1.875 \times 2.4\,\text{mm}^3$. The DTI acquisition time for a total of 3480 image slices was ~25 min, depending on subject heart rate.

Diffusion tensor image processing

All scans were transferred to a Linux Sun Ultra 40 workstation and processed with FSL 4.1.3 (http://www.fmrib.ox.ac.uk/fsl/) (Smith *et al.*, 2004). The DICOM files of each DTI acquisition were converted into a single multivolume NifTI file. This image was then corrected for eddy current distortion and movement artefact by affine registering every individual volume to the first $b=0$ volume. After this co-registration step the six $b=0$ volumes of each patient were extracted and averaged. A single investigator (M.Y.) used the average of the postoperative $b=0$ images to manually segment the surgical resection area in each patient, creating individual ROIs. Each ROI was then transformed into an inverse binary mask. The main diffusion

Table 1 Summary of the clinical characteristics of left and right temporal lobe epilepsy patients

	LTLE (range)	RTLE (range)
No of subjects	26	20
Sex—no. of males	10	8
Average age in years	37 (18–62)	37 (22–52)
Average age of epilepsy onset in years	9 (1–26)	10 (1–37)
Average duration of epilepsy in years	28 (8–60)	27 (6–47)
Average language lateralization index	−0.64 (−0.97–0.63)	−0.41 (−1–0.48)
Average surgical resection volume in mm³	21 087 (8809–30 761)	24 942 (10 368–39 025)
Average interval from surgery to scan in days	127 (90–193)	141 (85–351)
Number of patients of given ILAE class at time of postoperative scan	Class 1—21/81%	Class 1—14/70%
	Class 2—2	Class 2—1
	Class 3—1	Class 3—4
	Class 4—1	Class 4—1
	Class 5—1	
Average number of preoperative medications	2 (0–4)	2 (2–3)
Average number of postoperative medications	2 (1–4)	2 (1–3)

tensor and its eigenvalues ($\lambda_1, \lambda_2, \lambda_3$) and eigenvectors were then estimated for each voxel (Basser *et al.*, 1994), along with the summary parameters fractional anisotropy (FA) and mean diffusivity (MD) (Pierpaoli and Basser, 1996). By sorting the eigenvalues in the order of decreasing magnitude for each voxel ($\lambda 1 > \lambda 2 > \lambda 3$), $\lambda 1$ represents the diffusivity along the primary diffusion direction, that is, along the fibre axis, and is referred to as the axial diffusivity $\lambda \parallel$. The averaged water diffusivities perpendicular to the axonal fibres, $\lambda 2$ and $\lambda 3$ are referred to as $\lambda_T = (\lambda 2, + \lambda 3)/2$, or the radial diffusivity (Song *et al.*, 2002).

In order to align all FA data into a common space, the following procedure was applied separately for left and right TLE patients. First, all patients' preoperative FA data were aligned to the FMRIB58_FA standard space template supplied with FSL, using the nonlinear registration tool FNIRT (Andersson *et al.*, 2007*a*, *b*), which uses a b-spline representation of the registration warp field (Rueckert *et al.*, 1999). Secondly, each patient's postoperative FA image was co-registered to its preoperative FA image using the linear registration tool FLIRT (Jenkinson and Smith, 2001; Jenkinson *et al.*, 2002) and FNIRT. During this registration step the surgical ROI created from the postoperative $b = 0$ image was used to de-weight this area, such that the registration process ignores the information under the mask and prevents the surgically resected area contributing to the image registration (Brett *et al.*, 2001; Crinion *et al.*, 2007). Finally, the warps derived from each of the two steps were combined, and the resulting warp was applied to the native, postoperative FA image in each subject. In this manner, all pre- and postoperative data for subjects were aligned in a common space, and all images including postoperative data were re-sampled only once.

Following this, voxel-wise statistical analysis of the FA data was carried out in the left and right TLE groups separately, using TBSS (Smith *et al.*, 2006). The mean FA image across all pre- and postoperative images in each group was created, thinned and thresholded at FA > 0.2 to create a mean FA skeleton that represents the centres of all tracts common to the group (Smith *et al.*, 2006). Each patient's aligned FA and MD data were then projected onto this skeleton and the resulting data fed into voxel-wise cross-subject statistics.

In order to achieve accurate inference, including appropriate correction for multiple comparisons over space, we used permutation-based, non-parametric inference on a voxel-by-voxel basis (Nichols and Holmes, 2002). A paired *t*-test (5000 permutations) was used to assess the location and extent of significant increases and decreases in the FA and MD between pre- and postoperative scans in each group. Threshold-free cluster enhancement was used to correct results for multiple comparisons, and results were considered significant for $P < 0.05$. Threshold-free cluster enhancement is more sensitive than traditional cluster-based methods of thresholding and does not require the setting of an arbitrary, initial cluster-forming threshold or need a large amount of data smoothing (Smith and Nichols, 2009). Significant clusters were superimposed on the mean FA image and the MNI152 template supplied by FSL. FSLview and its atlas tools (International Consortium of Brain Mapping DTI-81 white matter labels atlas and John Hopkins University white matter probabilistic tractography atlas) in addition to general neuroanatomy atlases (Jackson and Duncan, 1996; Mori *et al.*, 2005) were used to anatomically label the location of significant clusters in MNI152 space.

In order to both validate and investigate our results further at an individual subject level, we de-projected and reverse-normalized significant clusters of changes in FA into their native pre- and postoperative images. Using these native clusters, mean pre- and postoperative FA, MD, $\lambda \parallel$ and λ_T values were calculated by masking the corresponding whole-brain diffusion parameter images with the clusters.

Pre- to postoperative percentage changes in each parameter in these clusters were then calculated using the equation above. These clusters were also masked with the $b = 0$ derived surgical masks in order to exclude those CSF-filled areas within the area of resection, which would confound the results.

Tractography

In order to assess the patterns of connections of selected clusters derived from the whole-brain analysis, fibre tracking was carried out using FMRIB's Diffusion toolbox (FDT) v2.0 (http://www.fmrib.ox.ac.uk/fsl/) (Smith *et al.*, 2004). In both groups, the diffusion characteristics were calculated in each voxel in each patient using a Markov chain Monte Carlo sampling method (Behrens *et al.*, 2003). In order to improve tractography in areas of crossing fibres, a two-tensor model was applied to the data (Behrens *et al.*, 2007). Probabilistic tracking was then seeded using the local maxima derived from the significant clusters obtained with the whole-brain TBSS analysis. Tracking was carried out in individual native space, and therefore, the seeding mask was deprojected and reverse-normalized before tracking was initiated. Tractography used default parameter settings (5000 iterations, 80 degrees curvature threshold) and tracts were thresholded at 10% of the number of streamlines generated. The resulting, thresholded, native space tracks were then spatially normalized by applying the same transformation matrix used to normalize the FA map in each patient. Tracts were then binarized and averaged to form a group map, which was superimposed upon the FSL MNI-152 T1 template with FSLview for the purpose of visualization. In these 'group variability' maps, each pixel reflects the percentage of subjects that contained a particular tract seeded with clusters derived from the whole-brain analysis. This approach enables the visualization of the consistency of the core of such tracts across a group of subjects.

Statistical analysis of clinical data and native clusters

Statistical analyses were performed with SPSS v14.0 (SPSS Inc. Chicago, IL, USA), and the threshold for statistical significance was set at $P < 0.05$. The normality of distribution of continuous, clinical variables was tested using the Kolmogorov–Smirnov test. Clinical variables (age, sex, age of onset of epilepsy, duration of epilepsy, resection volume, interval from surgery to postoperative scan, number of seizure-free patients at the time of postoperative scan, the average number of drugs before and after surgery) in left and right temporal lobe epilepsy groups were then compared using the independent samples *t*-test (continuous normally distributed variables), the Mann–Whitney U-test (continuous non-normally distributed variables) and the chi-squared exact test (categorical variables).

The Kolmogorov–Smirnov test was also used to test the distribution of all DTI-related native cluster parameters and the mean pre- and postoperative cluster diffusion parameters were compared using paired *t*-tests (continuous normally distributed variables), and the Wilcoxon signed ranks test (continuous non-parametrically distributed variables). The relationship between diffusion parameters, and Graded Naming Test and verbal fluency scores was assessed using Pearson's correlation test. A repeat partial correlation controlling for IQ and language laterality was also carried out.

Results

Clinical data

The clinical characteristics of the subjects studied are listed in Table 1. There were no significant differences in the age or duration of epilepsy of the left TLE and right TLE patients at the time of surgery, and no significant difference in the number of pre- or postoperative medications between left TLE and right TLE patients. The mean left anterior temporal lobe resection volume was 18% smaller than the mean right-sided resection [$t = -2.04$ (44), $P = 0.047$]. There were no significant differences in pre- and postoperative numbers of medications in either left TLE or right TLE patients. There was no significant difference in the age of onset, duration of epilepsy or interval from surgery to postoperative scan between left TLE and right TLE groups. There were no significant differences in either the gender distribution or number of patients seizure free at the time of postoperative scan.

Whole-brain analysis—left TLE patients

Following left anterior temporal lobe resection, there were significant decreases in FA in the main fibre tracts ipsilateral to the side of surgery, and also to a lesser extent in the contralateral hemisphere (Fig. 1). The areas of decreased FA corresponded to one contiguous, large cluster of 15 240 voxels ($P < 0.001$). The local maxima of this cluster were determined in order to investigate the anatomy of this cluster further (Table 2). The most significant decreases in FA were on the left side in the geniculo-calcarine tract and its projection to the lingual/occipital fusiform gyri, and intracalcarine cortex, part of the inferior longitudinal fasciculus, parahippocampal gyrus, crura of the fornix, anterior commissure and the anterior temporal portions of the superior longitudinal fasciculus. There were also significant decreases of FA in the temporal portion of the left uncinate fasciculus that connects to the temporal pole and the anterior floor of the external capsule. The latter structure contains fibres of the uncinate and inferior
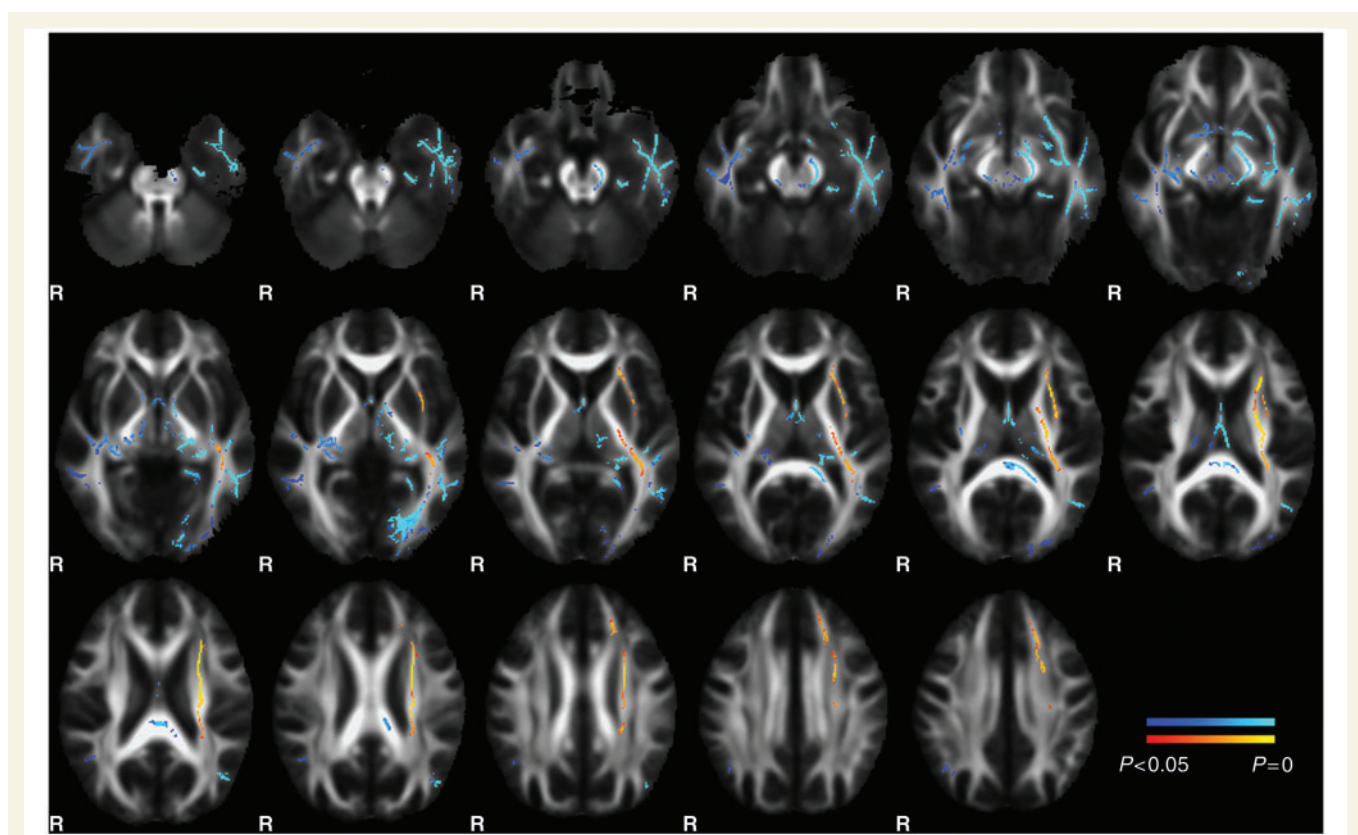
Figure 1 Threshold-free cluster-enhanced corrected ($P < 0.05$) results of the whole-brain tract-based spatial statistics analysis of fractional anisotropy after left anterior temporal lobe resection. The left side of the brain is on the right side of the image. R = right. Significant clusters representing increases (red to yellow) and decreases (blue to light blue) in fractional anisotropy after surgery are projected onto the mean fractional anisotropy template derived from all pre- and postoperative left temporal lobe epilepsy patients. For clarity, the group fractional anisotropy skeleton is not shown. The area of resection is visible inferiorly in the left temporal lobe where the white matter bundles are absent. Fractional anisotropy reduction after left anterior temporal lobe resection is apparent in the left temporal and occipital lobes, fornix, splenium and anterior commissure. There are also decreases in fractional anisotropy to a lesser extent in the contralateral hemisphere. Fractional anisotropy increases are present in the external capsule, posterior limb of the internal capsule and corona radiata. See Table 2 for more details regarding the anatomical location of local maxima.

Table 2 Summary of significant local maxima clusters found in whole-brain analysis of left TLE patients

Postoperative reduction of FA after left anterior temporal lobe resection	Left inferior longitudinal fasciculus ($P<0.001$) (may also contain fibres of left fronto-occpital fasciculus posteriorly)
	Right inferior longitudinal fasciculus—temporal portion ($P=0.025$)
	Left parahippocampal gyrus ($P<0.001$)
	Left cerebral peduncle ($P<0.001$) (containing cortico-pontine, cortico-spinal and cortico-bulbar fibres)
	Left uncinate fasciculus—temporal portion and portion lying on anterior floor of external capsule ($P<0.001$)
	Left inferior fronto-occipital fasciculus—portion lying in anterior floor of the external capsule superior to left uncinate fasciculus ($P<0.001$)
	Left fornix (crura and columns) ($P<0.001$)
	Right fornix (crura and columns) ($P<0.001$)
	Body of fornix ($P<0.001$)
	Left geniculo-calcarine tract ($P<0.001$)
	Splenium of corpus callosum/forceps major ($P<0.001$)
	Left superior longitudinal fasciculus—temporal portion connecting to superior and middle temporal gyri ($P<0.001$)
	Left anterior commissure ($P<0.001$)
	Right anterior commissure ($P=0.022$)
Postoperative increase in FA after left anterior temporal lobe resection	Right retrolenticular internal capsule ($P=0.021$)
	Left anterior corona radiata ($P=0.014$)
	Left posterior corona radiata ($P=0.006$)
	Left superior corona radiata ($P=0.006$)
	Left anterior–dorsal limb internal capsule ($P=0.001$)
	Left posterior limb internal capsule ($P=0.005$)
	Left retrolenticular region internal capsule ($P=0.015$)
	Left external capsule ($P=0.008$)
	Left superior frontal gyrus white matter ($P=0.014$)
	Left inferior frontal gyrus white matter ($P=0.013$)
Postoperative increase in MD after left anterior temporal lobe resection	Left inferior longitudinal fasciculus—temporal portion ($P<0.001$)
	Left uncinate fasciculus—temporal portion ($P<0.001$)
	Part of left anterior commissure ($P=0.014$)
	Left anterior floor external capsule—containing fibres of uncinate fasciculus and inferior fronto-occipital fasciculus ($P=0.03$)

Maximum P-values of local maxima clusters are given in brackets.

fronto-occipital fasciculi. Less-significant decreases in FA were also noted on the contralateral side in the fornix, anterior commissure and temporal portion of the inferior longitudinal fasciculus. Analysis of the de-projected, pre- and postoperative native clusters (Table 3) confirmed that there was a significant mean 7.08% decrease in FA in these areas postoperatively ($z=-3.845$, $P<0.001$) due mainly to a mean 7.77% increase in λ_T ($z=-3.883$, $P<0.001$). M.D. was also significantly increased by a mean 4.75% postoperatively in these areas ($z=-3.735$, $P<0.001$).

There were also widespread increases in FA evident an average of 4.5 months after left anterior temporal lobe resection, consisting of a single contiguous cluster of 3412 voxels ($P<0.001$) (Fig. 1). This cluster extended across a number of regions that included the anterior, posterior and superior corona radiata, the posterior limb (including the retrolenticular region) and dorsal part of the anterior limb of the internal capsule, and the external capsule (Table 2). Analysis of the deprojected, native pre- and postoperative clusters (Table 3) using paired t-tests confirmed a mean 7.84% postoperative increase in FA in this area [$t=-7.470$ (25), $P<0.001$]. This was due to a mean 2.95% postoperative increase in $\lambda \parallel$ [$t=-3.363$ (25), $P=0.002$] and a mean 4.74% decrease in λ_T [$t=3.336$ (25), $P=0.003$] (Table 3). There was no significant difference in MD values (mean −0.76%) in these clusters between pre- and postoperative patients.

Postoperative increases in MD were more limited consisting of a cluster of 2917 voxels ($P<0.001$). This cluster was restricted in distribution to those anterior portions of the inferior longitudinal fasciculus and uncinate fasciculus lying predominantly within the area of resection in patients (Supplementary Fig. 1 and Table 2). There were no significant decreases in MD after surgery.

Whole-brain analysis—right TLE patients

There were similar patterns of decreases in FA after right anterior temporal lobe resection, with a single significant cluster consisting of 19 248 voxels ($P<0.001$) (Fig. 2). The local maxima of this cluster are described in more detail in Table 4. Analysis of the pre- and postoperative de-projected, native cluster confirmed that there was a significant mean 6.76% reduction in FA in these areas ($z=-4.178$, $P<0.001$), which was predominantly due to a mean 8.43% increase in λ_T ($z=-3.709$, $P<0.001$) (Table 3). MD was also significantly increased postoperatively in these areas by a mean of 5.36% ($z=-3.467$, $P<0.001$) (Table 3).

The location of the increase in MD was similar to that seen after left anterior temporal lobe resection and consisted primarily of a cluster of 5850 voxels located within the surgical resection zone itself as well as its penumbra ($P<0.001$) (Supplementary Fig. 2).

Table 3 Summary of the mean diffusion parameters of back-normalized clusters identified from the whole-brain analysis

	Left TLE native cluster FA increase			Left TLE native cluster FA decrease			Right TLE native cluster FA decrease		
	Preoperative	Postoperative	Change (%)	Preoperative	Postoperative	Change (%)	Preoperative	Postoperative	Change (%)
FA (SE)	0.47 (0.006)	0.51 (0.007)	7.84 (1.06)	0.37 (0.006)	0.35 (0.005)	−7.08 (0.94)	0.39 (0.007)	0.36 (0.005)	−6.76 (1.12)
MD mm^{2}s^{-1} × 10^{-6} (SE)	770 (7.12)	764 (7.77)	−0.76 (1.06)	856 (20.10)	895 (18.90)	4.75 (1.08)	819 (11.90)	864 (17.90)	5.36 (0.98)
λ ‖ mm^{2}s^{-1} × 10^{-6} (SE)	1208 (12.22)	1242 (11.30)	2.95 (0.85)	1210 (18.67)	1226 (17.90)	1.42 (0.77)	1177 (10.46)	1203 (19.50)	2.13 (0.81)
λ_T mm^{2}s^{-1} × 10^{-6} (SE)	551 (6.70)	524 (8.17)	−4.74 (1.41)	680 (21.00)	730 (19.60)	7.77 (1.40)	640 (13.00)	694 (17.30)	8.43 (1.28)

Note in left and right TLE patients, the area of resection in each patient has been masked out so that results are not confounded by the CSF-filled surgical lacunae (SE = standard error).

In contrast to the effects of left anterior temporal lobe resection, there was a very limited pattern of postoperative FA increases after right anterior temporal lobe resection. A small, 255 voxel, peripheral white matter cluster within the anterior corona radiata was noted ($P < 0.001$) (Fig. 2). In view of the comparatively, small nature of this cluster, and its location in the periphery of the white matter skeleton, where mis-registration between scans is more likely, it was not analysed further. There were no significant postoperative decreases seen in MD using whole-brain analysis.

ROI analysis

In order to ensure that these results were not related to potential confounds associated with the realignment and spatial normalization of white matter tracts, we defined manual ROIs over the ipsilateral internal and external capsule on the raw, untransformed pre- and postoperative FA images of all patients who underwent left and right anterior temporal lobe resections. The ROIs were drawn over three consecutive axial slices beginning with the first slice in which the internal capsule could be clearly delineated from the external capsule. The anterior and posterior extents of the ROI were defined by lines tangential to the splenium and genu of the corpus callosum, respectively (Supplementary Fig. 3). After left anterior temporal lobe resection, there was a significant mean 5.80% increase in FA in this regions [$t = 3.709$ (25), $P = 0.001$]. In contrast, there was no significant change in FA in this region after right anterior temporal lobe resection.

Analysis of cluster of increased FA after left anterior temporal lobe resection

Having identified the increase in FA after left anterior temporal lobe resection, we explored potential artefactual causes for this finding. While scan–scan variability between pre- and postoperative acquisitions may confound results, previous assessments of such variability that have been carried out by our group suggest that this variability is of the order of 1–2% (Vollmar et al., 2010). This is significantly smaller than the changes observed in the present study. FA represents the degree of directionality of diffusion within individual voxels and is therefore higher in voxels containing a single-fibre population compared with two, crossing or kissing fibre populations. It is plausible, therefore, that if this cluster contains a predominance of voxels with two fibre bundles preoperatively, and one of these bundles is directly or indirectly connected to the area of resection, downstream Wallerian degeneration may cause an apparent increase in FA (Hoeft et al., 2007). We rejected this explanation as there was no significant difference in the proportion of voxels within the pre- and postoperative deprojected native clusters modelled as containing two fibre populations by the DTI processing.

An alternative explanation for the changes observed relates to the mechanical shift that can occur in the brain after surgery. Removal of the anterior temporal lobe may cause deformation of other parts of the brain, leading to stretching of nerve fibre bundles that may result in an increase in FA. If this hypothesis is correct, larger volumes of resection should cause greater shift in the remainder of the brain and potentially more stretching of
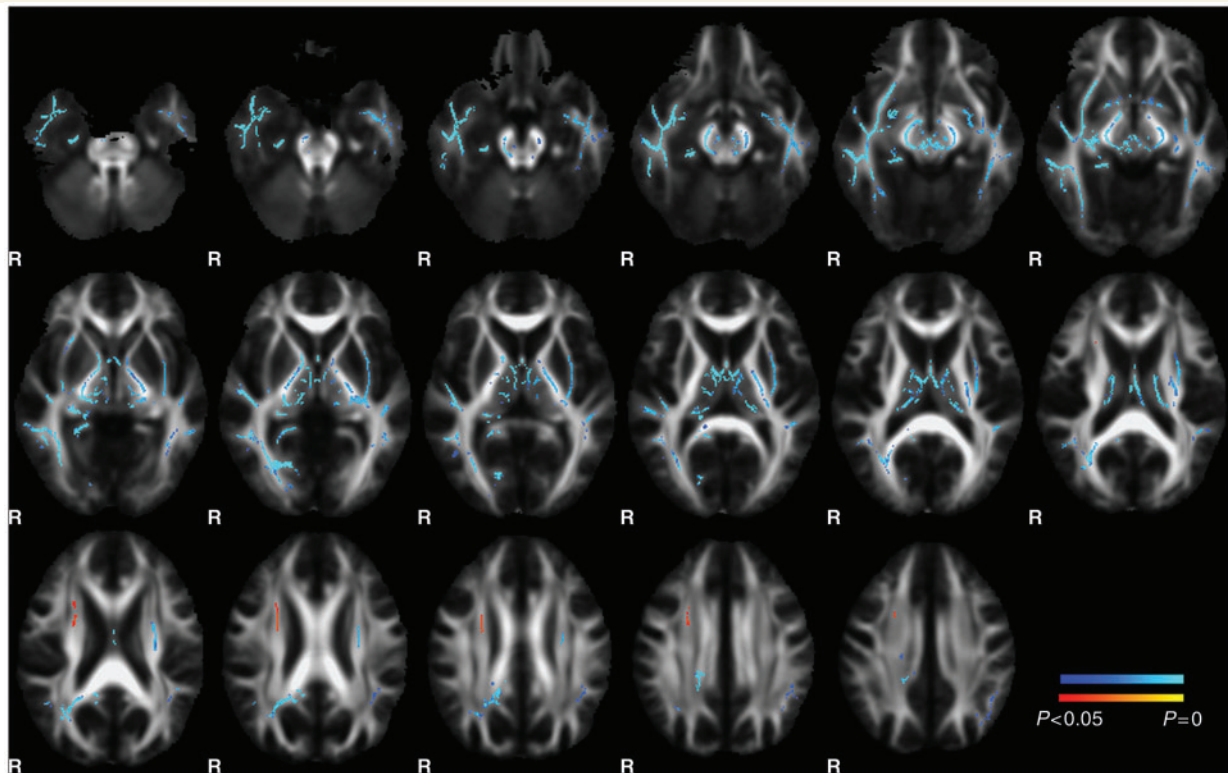
Figure 2 Threshold-free cluster-enhanced corrected ($P < 0.05$) results of the whole-brain tract-based spatial statistics analysis of fractional anisotropy after right anterior temporal lobe resection. The left side of the brain is on the right side of the image. R = right. Significant clusters representing increases (red to yellow) and decreases (blue to light blue) in fractional anisotropy are projected onto the mean fractional anisotropy template derived from all pre- and postoperative right temporal lobe epilepsy patients. For clarity, the group fractional anisotropy skeleton is not shown. The area of resection is visible inferiorly in the right temporal lobe where the white matter bundles are absent. Fractional anisotropy reduction after right anterior temporal lobe resection is apparent in the right temporal lobe, occipital lobe, fornix, splenium, anterior commissure and both cerebral peduncles. There are also decreases in fractional anisotropy to a lesser extent in the contralateral hemisphere. In comparison to patients undergoing a left anterior temporal lobe resection, there is only a very small area of increased fractional anisotropy in the anterior corona radiata.

white matter. We refuted this hypothesis as there was no significant correlation between the surgical resection volume and the percentage change in FA, $\lambda \parallel$ or λ_T after surgery. Further, the mean right anterior temporal lobe resection volume was greater than the equivalent resection on the left and the increases in FA were seen only after left-sided resections.

In order to assess the relationship of the increase in FA to seizure freedom and language, we stratified all patients undergoing a left anterior temporal lobectomy into several subgroups. These included seizure-free (ILAE Class I—21 patients) and non-seizure-free (ILAE Class II to IV—5 patients) groups at the time of their postoperative scan, and left (19 patients), bilateral (4 patients) and right (1 patients) hemisphere language dominant patients at the time of their surgery. A formal statistical comparison between the two groups is limited by the small numbers of patients in the non-seizure-free and right hemisphere dominant groups. However, both non-seizure-free and left hemisphere/bilaterally dominant patients had greater increases in FA compared with seizure-free (9.0% versus 7.4%) and right hemisphere dominant (7.6%/7.4% versus 3.9%) patients, respectively.

Verbal fluency and naming after left anterior temporal lobe resection and relationship to cluster of increased FA

As expected, there were significant correlations between the category and letter fluency scores preoperatively ($r = 0.689$, $P < 0.001$) and postoperatively ($r = 0.686$, $P < 0.001$), and between the percentage change in category and letter fluency after surgery ($r = 0.421$, $P = 0.020$). Three principal components were therefore extracted and used to represent pre- and postoperative verbal fluency and the percentage change in verbal fluency. There was no significant correlation between pre- or postoperative mean FA in this cluster and preoperative verbal fluency (Fig. 3A and B). However, there was a significant correlation between the pre- and postoperative mean FA in this cluster, and postoperative verbal fluency ($r = 0.482$, $P = 0.009$ and $r = 0.469$, $P = 0.010$, respectively) (Fig. 3C and D). These correlations remained significant after correction for IQ and language lateralization ($r = 0.443$, $P = 0.020$ and $r = 0.435$, $P = 0.022$).

This association was primarily underpinned by $\lambda \parallel$, and there was a correlation between percentage change in both verbal

Table 4 Summary of significant local maxima clusters found in whole-brain analysis of right TLE patients

Postoperative reduction of FA after right anterior temporal lobe resection	Right inferior longitudinal fasciculus ($P<0.001$) (may also contain fibres of left fronto-occpital fasciculus posteriorly)
	Left inferior longitudinal fasciculus ($P=0.013$) (may also contain fibres of left fronto-occpital fasciculus posteriorly)
	Right parahippocampal gyrus ($P<0.001$)
	Right cerebral peduncle ($P<0.001$) (containing cortico-pontine, cortico-spinal and cortico-bulbar fibres)
	Left cerebral peduncle ($P=0.012$) (containing cortico-pontine, cortico-spinal and cortico-bulbar fibres)
	Right uncinate fasciculus—temporal portion and portion lying on anterior floor of external capsule ($P<0.001$)
	Right inferior fronto-occipital fasciculus—portion lying in anterior floor of the external capsule superior to left uncinate fasciculus ($P<0.001$)
	Left external capsule ($P=0.012$)
	Right fornix (crura and columns) ($P<0.001$)
	Left fornix (crura and columns) ($P<0.001$)
	Body of fornix ($P<0.001$)
	Right geniculo-calcarine tract ($P<0.001$)
	Splenium of corpus callosum/forceps major ($P=0.015$)
	Right superior longitudinal fasciculus—temporal portion connecting to superior and middle temporal gyri ($P<0.001$)
	Right anterior commissure ($P<0.001$)
	Left anterior commissure ($P=0.013$)
	Left posterior limb of internal capsule ($P=0.012$)
Postoperative increase of FA after right anterior temporal lobe resection	Right superior corona radiata ($P=0.034$)
Postoperative increase in MD after right anterior temporal lobe resection	Right inferior longitudinal fasciculus—temporal portion ($P<0.001$)
	Right uncinate fasciculus—temporal portion ($P<0.001$)
	Part of right anterior commissure ($P=0.015$)
	Right anterior floor external capsule—containing fibres of uncinate fasciculus and inferior fronto-occipital fasciculus ($P=0.007$)
	Part of body of fornix ($P=0.029$)
	Right crura of fornix ($P=0.026$)
	Left crura of fornix ($P=0.026$)

Maximum *P*-values of local maxima clusters are given in brackets.

fluency and $\lambda \parallel$ after left anterior temporal lobe resection. That is, patients with the biggest increases in $\lambda \parallel$ after surgery had the smallest declines in verbal fluency ($r=0.398$, $P=0.027$). Again this correlation remained significant after correction for IQ and language lateralization ($r=0.457$, $P=0.016$). It should be noted that all of the above correlations remained significant when letter and category fluencies were considered separately.

There was also a significant correlation between pre- and post-operative $\lambda \parallel$ in this cluster and the postoperative graded naming test score ($r=0.388$, $P=0.030$ and $r=0.480$, $P=0.009$, respectively), but not the preoperative graded naming test score. In view of the apparent importance of $\lambda \parallel$, we tested for a correlation between the percentage increase in this parameter and the interval between temporal lobe resection and postoperative scanning. Although there was a positive trend this was not significant due to the presence of an outlier who was the only patient with an ILAE outcome of Class V in this group (Fig. 4). After exclusion of this outlier, this trend was significant ($r=0.400$, $P=0.024$), and the correlations between the diffusion parameters and verbal fluency and graded naming test scores remained significant.

In order to assess the specificity of these correlations we also calculated the global, mean pre- and postoperative FA across the whole brain. Neither of these measures correlated with pre- or postoperative verbal fluency or graded naming test scores. Furthermore, there was no correlation between the global percentage change in $\lambda \parallel$ and the interval between temporal lobe resection and postoperative scanning.

Tractography

Postoperative tractography from those areas demonstrating an increase in FA after surgery in left anterior temporal lobe resection is shown in Fig. 5. The group variability map of this network of connections consisted of two predominant pathways. Firstly, there was a network of connections running from the precentral gyrus, through the posterior limb of the internal capsule limb to the corticospinal tract and pons. The second pathway consisted of connections from premotor and prefrontal areas, the superior and inferior frontal gyrus (including the deep frontal operculum), and passed via the external capsule to the posterior, superior temporal gyrus and angular gyrus. As this pathway passes through the external capsule, it is ventral and medial to the arcuate fasciculus/superior longitudinal fasciculus whose anatomical location is also shown in Fig. 5 for reference. Part of the distribution of the group variability maps (Fig. 5) approximates to the ventro-medial language network that is distinguishable from the arcuate
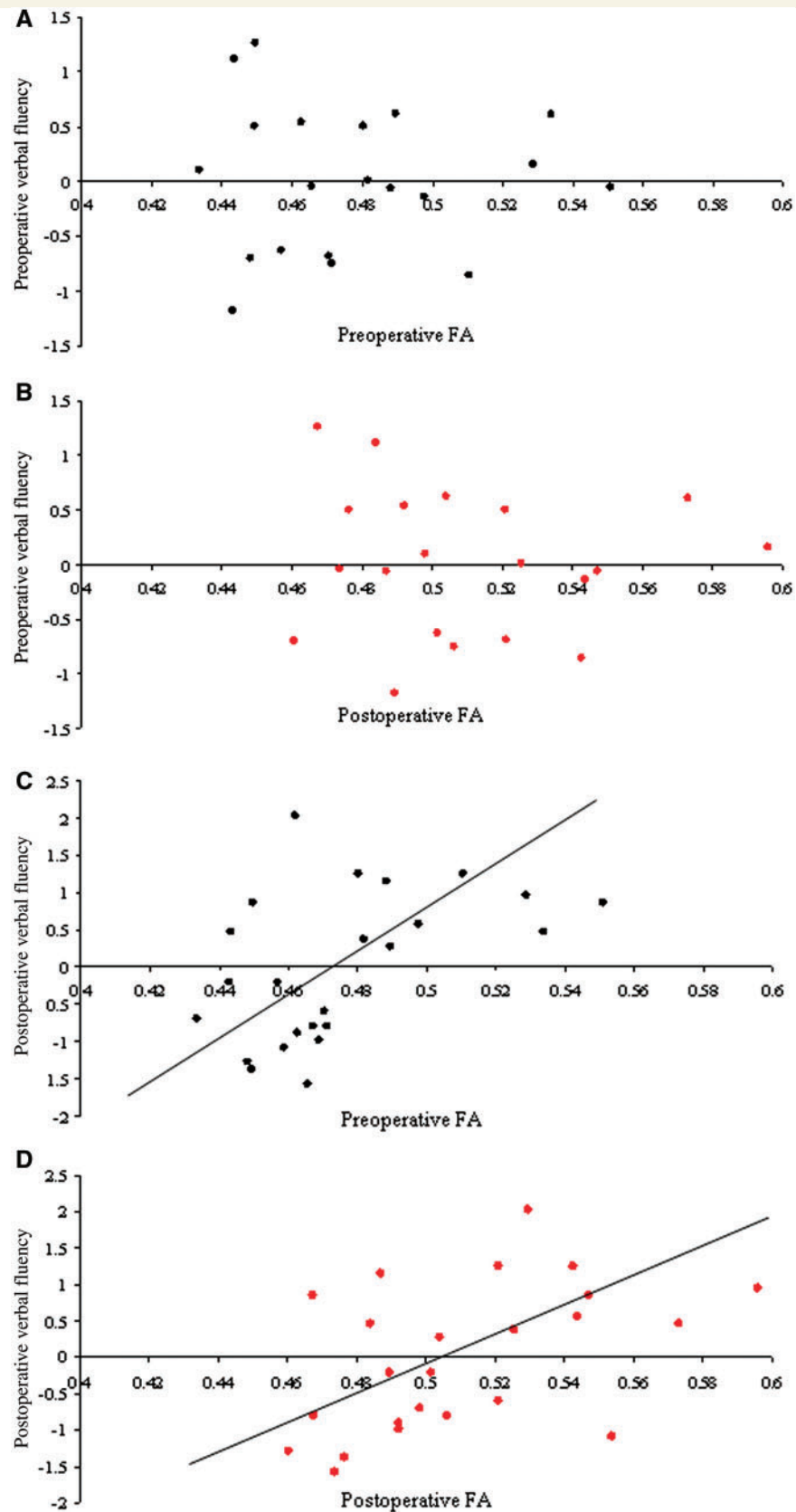
Figure 3 Scatterplots of verbal fluency scores against the mean fractional anisotropy in left posterior limb internal capsule, external capsule and corona radiata before (black dots) and after (red dots) left anterior temporal lobe resection. There was a significant correlation between the mean fractional anisotropy in this cluster before and after left anterior temporal lobe resection, and postoperative verbal fluency ($r = 0.482$, $P = 0.009$ and $r = 0.469$, $P = 0.010$, respectively) (Fig. 3**C** and **D**) but not pre-operative verbal fluency scores (Fig. 3**A** and **B**).
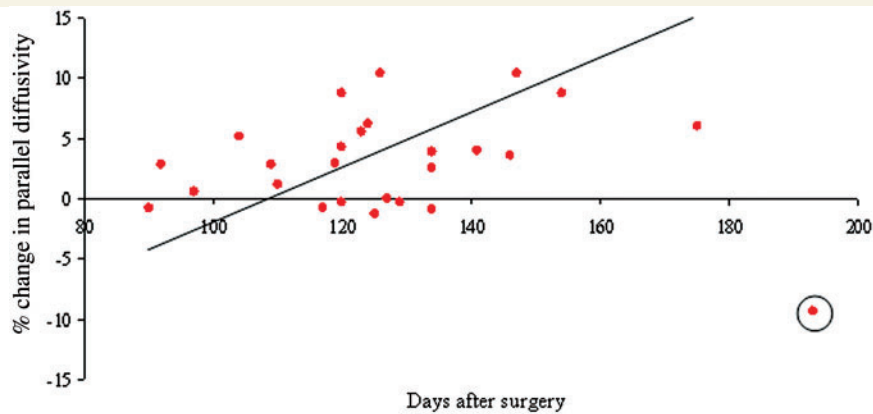
Figure 4 Scatterplot and regression line of percentage change in λ ‖ in the cluster showing an increase in fractional anisotropy after left anterior temporal lobe resection against interval between surgery and imaging. The circled point is an outlier, and when removed from the analysis, the correlation is significant ($r = 0.400$, $P = 0.024$).
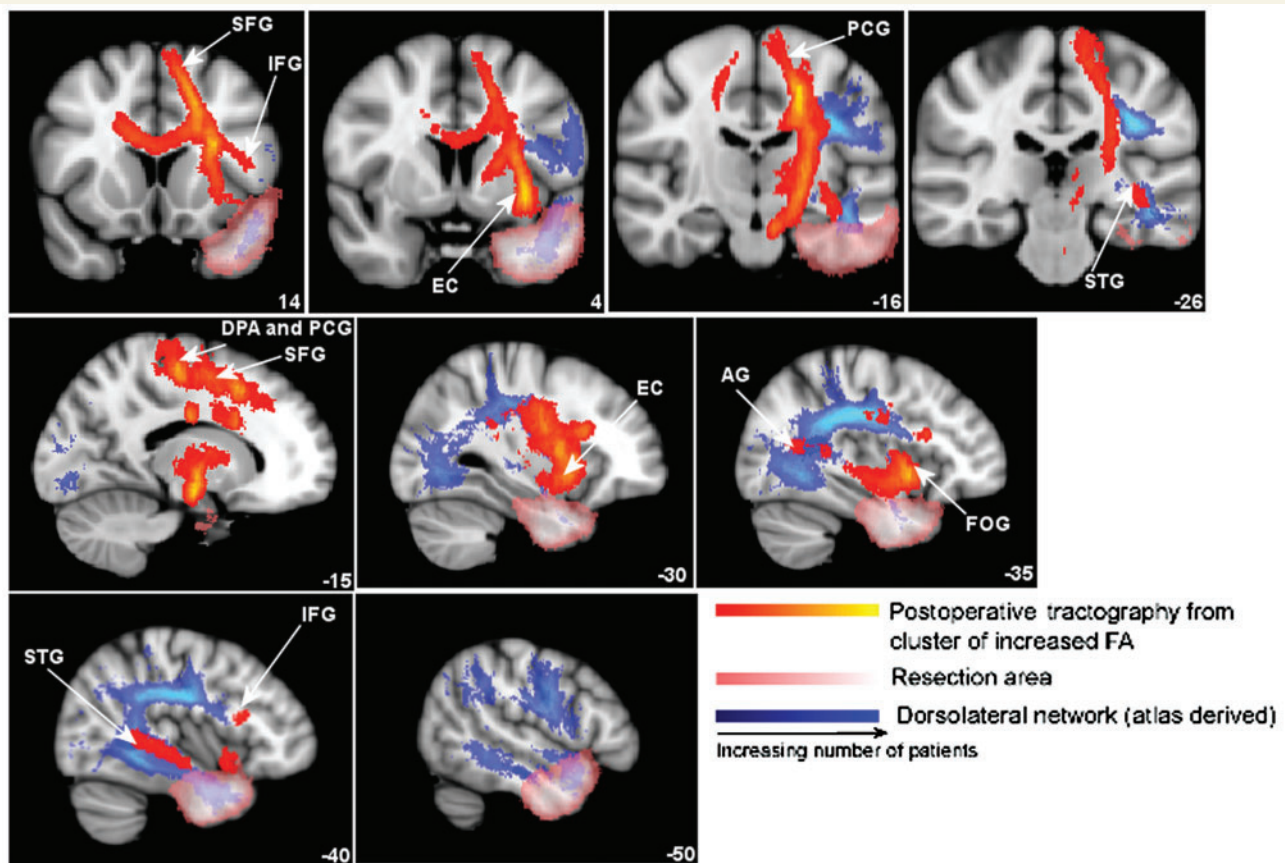
Figure 5 Group variability map (thresholded at 0.2) of tractography results after seeding from the local maxima of the cluster identified as showing an increase in fractional anisotropy after left anterior temporal lobe resection. Tracts are superimposed upon the MNI152_T1_1mm_brain image supplied with FSL. The group variability map (yellow–red, with yellow representing voxels identified by the tractography in all subjects) visualizes connections from the precentral gyrus via the internal capsule, and connections from the premotor and prefrontal areas, the superior and inferior frontal gyrus (including the deep frontal operculum), which pass via the external capsule to the posterior, superior temporal gyrus and angular gyrus. This network of connections is medial to the traditional dorso-lateral language pathway composed of the arcuate fasciculus and inferior longitudinal fasciculus. The latter pathway is shown for reference in blue and is derived from the JHU white matter tractography atlas supplied with FSL. Also shown is the group variability map for the surgical resection area (dark pink to light pink) created from the postoperative $b = 0$ images (thresholded at 0.3). It is evident that after an anterior temporal lobe resection the dorso-lateral language connections may be more susceptible to resection and damage than the ventro-medial connections. MNI coordinates are shown on each slice. (DPA = dorsal premotor area; PCG = precentral gyrus; SFG = superior frontal gyrus; EC = external capsule; AG = angular gyrus; FOG = fronto-orbital gyrus; STG = superior temporal gyrus; IFG = inferior frontal gyrus).

fasciculus/superior longitudinal fasciculus, which make up the dorso-lateral language network (Saur *et al.*, 2008).

Discussion

This study demonstrates the structural consequences of anterior temporal lobe resection on white matter networks in patients with temporal lobe epilepsy. Areas of decreased FA and increased MD were evident after both left- and right-sided resections.

There were also significant focal postoperative increases in FA after left anterior temporal lobe resections. The location of these changes, their correlation with language function and presence only after left-sided temporal lobe surgery and with greater increases occurring after longer intervals from surgery suggest that they may be related to structural plasticity relevant to language function after surgery. This information is likely to be important for the planning of epilepsy surgery and prediction of postoperative language function, and for the understanding of brain recovery following injury.

Postoperative reduction in FA

Three published studies have assessed the structural consequences of epilepsy surgery on white matter (Concha *et al.*, 2006, 2007; Schoene-Bake *et al.*, 2009). Schoene-Bake *et al.* carried out a TBSS analysis of diffusion data of 21 right and 19 left temporal lobe epilepsy patients. All but two of the patients underwent a selective amygdalo-hippocampectomy. Healthy controls were used as a comparison group for postoperative patients due to lack of preoperative data. Overall, the distribution of reduction in FA was similar to the current study, both ipsilaterally and contralaterally, although we have observed more extensive changes postoperatively. This is not surprising given that anterior temporal lobe resection removes more brain tissue than an amygdalo-hippocampectomy, and the lack of preoperative data in the Schoene-Bake *et al.*'s study (2009).

Decreased FA can be caused by decreased diffusivity parallel to axonal fibres or by increased perpendicular diffusivity (Beaulieu, 2002; Chahboune *et al.*, 2009). In the present study, the decrease in FA in those white matter networks connected to the area of resection was caused by an increase in λ_T that was relatively larger than the decrease in FA. Concha *et al.* assessed the effects of a corpus callostomy in three subjects, and reported similar findings (Concha *et al.*, 2006). The changes in diffusion parameters after surgery evolved from an acute pattern ~1 week after surgery, to a more chronic pattern several months after surgery. The biggest and most significant reductions in FA were closest to the surgical lesion. In the present study, the contralateral reductions in FA, which were furthest from the area of resection, also appear to be less marked than those areas close to the area of resection. Electron microscopy studies of the basis of reduced FA have proposed that increases in λ_T are caused by reduced axonal density and increased extra-axonal fraction (Hui *et al.*, 2007; Concha *et al.*, 2010) or decreased myelin (Gulani *et al.*, 2001; Harsan *et al.*, 2006). In the present study, the decrease in FA is likely to be related to Wallerian degeneration of nerve bundles disconnected from afferent and/or efferent structures, which in turn may cause myelin degradation and decreased axonal packing. Concha *et al.* (2006) also reported a chronic increase in $\lambda \parallel$, which we observed. Based on the evidence from animal models, in this context, this may be due to loss of axons and intra-axonal structures such as neurofilaments and microtubules, thereby reducing the barriers to parallel diffusivity (Kinoshita *et al.*, 1999). Overall, the increase in λ_T and $\lambda \parallel$ also give rise to an increase in MD in those areas identified as showing a decrease in FA after surgery.

Postoperative increase in FA

We observed extensive postoperative increases in FA after left anterior temporal lobe resection, which has not been reported previously after adult epilepsy surgery (Concha *et al.*, 2006, 2007; Schoene-Bake *et al.*, 2009). In both studies by Concha *et al.* patient numbers were small, and the ROI approach used limits investigation to *a priori* defined regions. However, one of the regions assessed included the external capsule (Concha *et al.*, 2007). Though the authors did not report significant postoperative increases in FA in this region, their data suggest a trend towards a postoperative increase in FA underpinned by an increase in $\lambda \parallel$ and decrease in λ_T. In the study by Schoene-Bake *et al.*, the lack of preoperative data may have reduced the sensitivity to detect postoperative increases in FA. Finally, the patients assessed in these three studies predominantly underwent selective amygdalo-hippocampectomy, and not anterior temporal lobe resection. In the current investigation, the longitudinal design with pre- and postoperative data, the whole-brain analysis techniques and a relatively large number of patients undergoing anterior temporal lobe resection enabled detection of increases in FA, and an ROI analysis of the raw data confirmed these findings. This supposition is supported by a recent study, which assessed white matter changes after hemispherectomy in 10 children (Govindan *et al.*, 2009). The authors of this longitudinal study used a TBSS-based analysis, and reported an increase in FA in the contralateral corona radiata, which also correlated with time after surgery.

The postoperative increase in FA in the present study was caused by both an increase in $\lambda \parallel$ and a decrease in λ_T. For this reason the MD of this cluster was unchanged postoperatively. There are several potential causes of these observed changes. We demonstrated that mechanical stretch of white matter tracts or a decrease in the proportion of voxels modelled as containing two fibre bundles is unlikely to be a contributing factor. The widespread distribution of the increase in FA, the lack of similar changes after right anterior temporal lobe resections and the absence of a correlation between resection volume and percentage change in diffusion parameters argue against these possible explanations. Furthermore, while stretching of white matter bundles may explain a decrease in λ_T due to increased axonal packing, this would not explain the increase in $\lambda \parallel$, which tends to decrease with reduced axonal calibre (Harsan *et al.*, 2006; Wu *et al.*, 2007).

Postoperative increases in FA could also be due to seizure cessation after surgery. Concha *et al.* found persistent bilateral white

matter diffusion changes postoperatively and proposed that these were probably secondary to irreversible structural damage such as myelin degradation and axonal degeneration. However, they also acknowledged that Wallerian degeneration related to surgery may mask structural changes associated with functional recovery (Concha *et al.*, 2007). More recently, Yasuda *et al.* carried out a whole-brain VBM comparison of pre- and postoperative T_1-weighted data in 67 patients with TLE (Yasuda *et al.*, 2009). The authors identified significant increases in white matter concentration in the ipsilateral temporal and frontal lobes after temporal lobe surgery, with a distribution similar to that observed in the present study. However, because both left and flipped right TLE patients were analysed together, it is impossible to ascertain whether there were differences in these increases in left and right TLE groups. The authors suggested that these findings were a consequence of seizure cessation in association with reversible metabolic dysfunction and neuronal plasticity. That interpretation is in keeping with several PET and MR spectroscopy studies that have suggested postoperative reversal of preoperative, extra-temporal metabolic dysfunction in TLE (Hugg *et al.*, 1996; Cendes *et al.*, 1997; Spanaki *et al.*, 2000; Joo *et al.*, 2005). There is also evidence that the cortical and sub-cortical networks underlying propagation of secondarily generalized seizures predominate between the mid-brain, basal ganglia and thalamus (Blumenfeld *et al.*, 2009). The white matter connecting these structures consists primarily of sub-cortical tracts that pass through the internal capsule and corona radiata (Schmahmann and Pandya, 2008) and is broadly consistent with the location of the increases in FA identified in the present study. Despite this, our observation that seizure-free patients had smaller mean increases in FA than non-seizure-free patients suggests that seizure freedom is not the primary cause of increased FA observed after surgery. Rather, the location of these increases in FA confined to left temporo-frontal white matter tracts, and the observation that left hemisphere language-dominant patients have larger increases in FA after left temporal lobe surgery than right hemisphere dominant patients suggests that the major cause of these changes may be related to the structural plasticity of language networks after anterior temporal lobe resection.

Language and structural plasticity

Advanced magnetic resonance imaging techniques and analyses have shown that there is considerable capacity for, not only functional but also structural, reorganization after brain injury in the adult human brain (May and Gaser, 2006; Gould, 2007; Johansen-Berg, 2007; Draganski and May, 2008). Traditional tract-tracing techniques in animal models have highlighted the central role of white matter reorganization in this process (Kaas *et al.*, 1999; Jain *et al.*, 2000; Dancause *et al.*, 2005), and diffusion-based MRI techniques corroborate these findings. For example, studies of patients with blindsight highlight the scope of white matter reorganization underlying preservation of visual abilities after occipital cortical lesions (Leh *et al.*, 2006; Bridge *et al.*, 2008). Similarly, studies of animal models of spinal cord injury demonstrate the correlation between diffusion MRI-derived

measurements and immunohistological markers of plasticity (Ramu *et al.*, 2008).

The premise that the postoperative increases in FA after left anterior temporal lobe resection may be related to the plasticity of language networks after surgery is substantiated for two reasons; the location of these changes is in keeping with the current understanding of the neuro-anatomical basis of language, and there are significant correlations between independent neuro-psychometric data and the mean diffusion parameters derived from these clusters. Models of language postulate the existence of an expressive language area in the left ventrolateral frontal region (Broca's area) (Grodzinsky and Amunts, 2006),which is connected to temporo-parietal language regions via the arcuate fasciclus (Geschwind, 1970). Recent diffusion-based MRI studies suggest that the arcuate fasciculus has much more extensive putative cortical terminations beyond the classical limits of Broca's and Wernicke's area, to include the dorsal premotor cortex, the dorso-lateral prefrontal cortex and the anterior middle and inferior temporal gyri (Catani *et al.*, 2005; Frey *et al.*, 2008; Glasser and Rilling, 2008; Bernal and Altman, 2009). Furthermore, tract-tracing studies in primates suggest that the arcuate fasciculus is not a single, direct, white matter connection between frontal and temporo-parietal regions, but instead is part of a dorsal stream of connections that includes parts of the superior longitudinal fasciculus and the middle and inferior longitudinal fascicule (Schmahmann and Pandya, 2006; Frey *et al.*, 2008; Saur *et al.*, 2008). Current standard tractography techniques do not have the spatial resolution needed to resolve these corticocortical pathways (Frey *et al.*, 2008). However, these connections have been visualized in humans and primates using high-resolution diffusion techniques (Makris *et al.*, 2005, 2009; Schmahmann *et al.*, 2007). These studies have also identified a second, parallel, ventral language circuit that is located medial to this dorsal pathway. This runs from the ventrolateral prefrontal and orbitofrontal cortex, and inferior and middle frontal gyri, through the extreme capsule dorsal to the uncinate fasciculus, to the posterior/middle superior temporal gyri, where it merges with the fibres of the middle longitudinal fasciculus, which is lateral to it and connects to the inferior parietal lobe and angular gyrus (Petrides and Pandya, 1984, 1988, 2006, 2007; Frey *et al.*, 2008; Saur *et al.*, 2008; Makris and Pandya, 2009). Current *in vivo* diffusion tensor imaging lacks the spatial resolution to unambiguously differentiate between the external and extreme capsules by means of FA maps alone. For this reason, the postoperative increases in FA appear to be localized to the external capsule of the TBSS skeleton in the present study. However, tractography seeded from these areas demonstrates the presence of connections linking temporo-parietal areas with the ventral prefrontal areas, and inferior frontal gyrus, which is consistent with the ventro-medial language pathway (Fig. 5). The other morphological features identified by the postoperative tractography in this study are also concordant with the current understanding of language networks, including connections from the dorsal prefrontal areas, superior frontal gyrus, precentral gyrus and premotor areas, which overlap with parts of the dorsal language network and connect to parts of the basal ganglia. These areas are likely to be important for final speech production, and

higher order articulatory control of speech (Duffau, 2008; Frey et al., 2008).

Damage to this distributed network may occur following left anterior temporal lobe resection and is most likely to affect the dorsal rather than ventro-medial pathway because of the former's lateral position, and the anterior extent of fibres connecting to the superior and middle/inferior temporal gyri. In contrast, the ventral pathway is more medial and connects to the posterior/middle superior temporal gyrus (Fig. 5) and may therefore be less susceptible to injury (Moran et al., 1999). This ventro-medial pathway may therefore have a greater propensity to undergo plasticity-related changes relevant to language functioning after surgery. This contention is substantiated by the presence of significant correlations between pre- and postoperative mean FA and $\lambda_\parallel$ values and postoperative verbal fluency and naming scores, but not pre-operative scores. It appears that the most significant component of this correlation is the increase in $\lambda_\parallel$ after surgery, demonstrated by the correlation between the percentage change in $\lambda_\parallel$ and the percentage change in verbal fluency after left anterior temporal lobe resection. Whilst there is debate as to the specific role of each pathway with respect to language functions (Friederici, 2009), some functional overlap seems likely with both pathways contributing to a high proficiency in verbal communication (Saur et al., 2008). The biological interpretation of a pattern of increased $\lambda_\parallel$ in concert with decreased λ_T is not well defined, but may be primarily related to an increase in myelination (DeBoy et al., 2007) in addition to an increase in axonal calibre (Wu et al., 2007) and neurofilament density (Sun et al., 2008).

The predominance of the ipsilateral, rather than contralateral, white matter network with respect to language function after surgery is corroborated by the few longitudinal studies that have assessed the functional reorganization of language after epilepsy surgery (Pataraia et al., 2005; Helmstaedter et al., 2006; Wong et al., 2009). Although these studies have used differing methods, they all highlight the importance of the ipsilateral hemisphere (Helmstaedter et al., 2006; Wong et al., 2009) and intra-hemispheric reorganization of language after dominant temporal lobe resection (Pataraia et al., 2005). The study by Pataraia et al. also demonstrated ipsilateral inferior displacement of receptive language activation after anterior temporal lobe resection (Pataraia et al., 2005). Furthermore, larger studies in patients with other forms of brain injury, such as stroke, also support that it is the repair and strengthening of ipsilateral, neighbouring networks that is more important, than the recruitment of contra-lateral homologous regions (Saur et al., 2006).

The current study suggests a structural correlate to the concept of ipsilateral reorganization and recovery of function, with augmentation of the ventro-medial language network, consequent to surgical damage to the dorsal–lateral language pathway. We suggest that the focal increases in FA seen in the ventro-medial language network after left anterior temporal lobe resection represents an attempt to reorganize language function after brain injury caused by surgery. Importantly, the observed correlation between preoperative diffusion parameters and postoperative language outcome suggests that the preoperative state of the ventro-medial language network is important, and that if this network is already in 'active service', left anterior temporal lobe

resection will have less impact on language functioning. Further studies are needed to clarify whether diffusion imaging and tractography of this ventral network might provide predictive information regarding the risk of language dysfunction after anterior temporal lobe resection, and moreover whether it can provide functional landmarks that can be used to guide surgery in order to minimize postoperative language dysfunction. Further longitudinal investigations with more time points following surgery will clarify the time course of these changes in FA, and these studies are ongoing.

Limitations

Whole brain and tractography methods of analysis of diffusion data have several limitations. The presence of brain lesions can cause problems with the normalization of images to standard space when using whole-brain methods. We have attempted to minimize these complications by registering the postoperative images to their preoperative counterparts using hand drawn cost function masks over the areas of resection, before normalizing all images to a common space. We incorporated this method within the framework of TBSS that is specifically optimized for the registration of diffusion data. The confirmation of our whole-brain findings, using native cluster information, and hand-drawn ROIs lends confidence to the robustness of the methods employed in this study. The resolution of tractography images is several orders of magnitude lower than the nerve bundles under examination. A single voxel contains numerous fibre populations, some of which may be kissing or crossing, and this is particularly problematic in the fronto-temporo-parietal areas assessed in this study. Although, the multiple fibre model, and probabilistic tractography approach employed in this study, may be able to partly deal with these problems, ultimately higher resolution in vivo diffusion imaging techniques are needed to precisely delineate the many subcomponents of the language network. The delineation of individual white matter tracts connecting different, language relevant cortical areas, in association with functional data, should facilitate a better understanding of the functional specificity of these white matter subcomponents. The use of a language laterality index derived from an expressive, rather than receptive, fMRI task that activates the frontal lobe may also be a limiting factor, given that the targeted surgical area is the temporal lobe. However, though it might be useful to have a measure of receptive language function, crossed dominance is uncommon and damage to white matter tracts after surgery is as likely to affect frontal, as well as temporal, lobe functioning (Catani, 2007). Further, the language deficit encountered after anterior temporal lobe resection is commonly of word finding, and not of receptive function (Barr, 2009). The correlations between neuropsychology and diffusion data noted in this study were not corrected for multiple comparisons due to the small numbers of patients studied. However, even with an adjusted Bonferroni significance level of 0.05/4, the correlations remain significant, and the broad theme of this study is consistent.

Conclusion

We have used whole-brain voxel-based analysis of diffusion tensor imaging to assess the morphometric changes in white matter

following left and right anterior temporal lobe resection. While widespread decreases in FA occurred after left- and right-sided resections, only the left anterior temporal lobe resections were followed by an increase of FA in an extensive area. The location of these changes and the results of tractography seeded from this area suggest that it may be part of a parallel, ventro-medial language network. This is corroborated by a significant correlation between the diffusion parameters of this region and postoperative language function. These findings have important implications for our understanding of the response of the brain to injury and may prove useful in the planning of epilepsy surgery in order to minimize postoperative language dysfunction.

Acknowledgements

Funding

Supplementary material

Supplementary material is available at *Brain* online.

References

Andersson JLR, Jenkinson M, Smith S. Non-linear optimisation. FMRIB Technical Report. FMRIB Center, 2007b.

Andersson JLR, Jenkinson M, Smith S. Non-linear registration, aka spatial normalisation. FMRIB Technical Report. FMRIB Center, 2007a.

Backes WH, Deblaere K, Vonck K, Kessels AG, Boon P, Hofman P, et al. Language activation distributions revealed by fMRI in post-operative epilepsy patients: differences between left- and right-sided resections. Epilepsy Res 2005; 66: 1–12.

Barr WB. Neuropsychological outcome. In: Luders H, editor. Textbook of epilepsy surgery. London: Informa Healthcare; 2009. p. 1277–99.

Basser PJ. Inferring microstructural features and the physiological state of tissues from diffusion-weighted images. NMR Biomed 1995; 8: 333–44.

Basser PJ, Mattiello J, LeBihan D. MR diffusion tensor spectroscopy and imaging. Biophys J 1994; 66: 259–67.

Beaulieu C. The basis of anisotropic water diffusion in the nervous system - a technical review. NMR Biomed 2002; 15: 435–55.

Behrens TE, Berg HJ, Jbabdi S, Rushworth MF, Woolrich MW. Probabilistic diffusion tractography with multiple fibre orientations: What can we gain? Neuroimage 2007; 34: 144–55.

Behrens TE, Woolrich MW, Jenkinson M, Johansen-Berg H, Nunes RG, Clare S, et al. Characterization and propagation of uncertainty in diffusion-weighted MR imaging. Magn Reson Med 2003; 50: 1077–88.

Bernal B, Altman N. The connectivity of the superior longitudinal fasciculus: a tractography DTI study. Magn Reson Imaging 2009; 28: 217–25.

Blumenfeld H, Varghese GI, Purcaro MJ, Motelow JE, Enev M, McNally KA, et al. Cortical and subcortical networks in human secondarily generalized tonic-clonic seizures. Brain 2009; 132: 999–1012.

Brett M, Leff AP, Rorden C, Ashburner J. Spatial normalization of brain images with focal lesions using cost function masking. Neuroimage 2001; 14: 486–500.

Bridge H, Thomas O, Jbabdi S, Cowey A. Changes in connectivity after visual cortical brain damage underlie altered visual function. Brain 2008; 131: 1433–44.

Briellmann RS, Mitchell LA, Waites AB, Abbott DF, Pell GS, Saling MM, et al. Correlation between language organization and diffusion tensor abnormalities in refractory partial epilepsy. Epilepsia 2003; 44: 1541–5.

Catani M. From hodology to function. Brain 2007; 130: 602–5.

Catani M, Jones DK, ffytche DH. Perisylvian language networks of the human brain. Ann Neurol 2005; 57: 8–16.

Cendes F, Andermann F, Dubeau F, Matthews PM, Arnold DL. Normalization of neuronal metabolic dysfunction after surgery for temporal lobe epilepsy. Evidence from proton MR spectroscopic imaging. Neurology 1997; 49: 1525–33.

Chahboune H, Mishra AM, DeSalvo MN, Staib LH, Purcaro M, Scheinost D, et al. DTI abnormalities in anterior corpus callosum of rats with spike-wave epilepsy. Neuroimage 2009; 47: 459–66.

Cheung MC, Chan AS, Lam JM, Chan YL. Pre- and postoperative fMRI and clinical memory performance in temporal lobe epilepsy. J Neurol Neurosurg Psychiatry 2009; 80: 1099–106.

Concha L, Beaulieu C, Wheatley BM, Gross DW. Bilateral white matter diffusion changes persist after epilepsy surgery. Epilepsia 2007; 48: 931–40.

Concha L, Gross DW, Wheatley BM, Beaulieu C. Diffusion tensor imaging of time-dependent axonal and myelin degradation after corpus callosotomy in epilepsy patients. Neuroimage 2006; 32: 1090–9.

Concha L, Livy DJ, Beaulieu C, Wheatley BM, Gross DW. In vivo diffusion tensor imaging and histopathology of the fimbria-fornix in temporal lobe epilepsy. J Neurosci 2010; 30: 996–1002.

Cook PA, Symms M, Boulby PA, Alexander DC. Optimal acquisition orders of diffusion-weighted MRI measurements. J Magn Reson Imaging 2007; 25: 1051–8.

Crinion J, Ashburner J, Leff A, Brett M, Price C, Friston K. Spatial normalization of lesioned brains: performance evaluation and impact on fMRI analyses. Neuroimage 2007; 37: 866–75.

Dancause N, Barbay S, Frost SB, Plautz EJ, Chen D, Zoubina EV, et al. Extensive cortical rewiring after brain injury. J Neurosci 2005; 25: 10167–79.

DeBoy CA, Zhang J, Dike S, Shats I, Jones M, Reich DS, et al. High resolution diffusion tensor imaging of axonal damage in focal inflammatory and demyelinating lesions in rat spinal cord. Brain 2007; 130: 2199–210.

Draganski B, May A. Training-induced structural changes in the adult human brain. Behav Brain Res 2008; 192: 137–42.

Duffau H. The anatomo-functional connectivity of language revisited. New insights provided by electrostimulation and tractography. Neuropsychologia 2008; 46: 927–34.

Duncan JS. Imaging and epilepsy. Brain 1997; 120(Pt 2): 339–77.

Engel J Jr. Etiology as a risk factor for medically refractory epilepsy: a case for early surgical intervention. Neurology 1998; 51: 1243–4.

Focke NK, Yogarajah M, Bonelli SB, Bartlett PA, Symms MR, Duncan JS. Voxel-based diffusion tensor imaging in patients with mesial temporal

lobe epilepsy and hippocampal sclerosis. Neuroimage 2008; 40: 728–37.

Frey S, Campbell JS, Pike GB, Petrides M. Dissociating the human language pathways with high angular resolution diffusion fiber tractography. J Neurosci 2008; 28: 11435–44.

Friederici AD. Pathways to language: fiber tracts in the human brain. Trends Cogn Sci 2009; 13: 175–81.

Geschwind N. The organization of language and the brain. Science 1970; 170: 940–4.

Glasser MF, Rilling JK. DTI tractography of the human brain's language pathways. Cereb Cortex 2008; 18: 2471–82.

Gould E. How widespread is adult neurogenesis in mammals? Nat Rev Neurosci 2007; 8: 481–8.

Govindan RM, Chugani HT, Altinok D, Sood S. Postsurgical white matter changes identified using diffusion tensor imaging in children following hemispherectomy. Epilepsia 2009 (Abstracts from the 2009 Annual Meeting of the American Epilepsy Society); (Suppl. 11): 1–502.

Grodzinsky Y, Amunts K. Broca's region. New York: Oxford University Press; 2006.

Gulani V, Webb AG, Duncan ID, Lauterbur PC. Apparent diffusion tensor measurements in myelin-deficient rat spinal cords. Magn Reson Med 2001; 45: 191–5.

Harsan LA, Poulet P, Guignard B, Steibel J, Parizel N, de Sousa PL, et al. Brain dysmyelination and recovery assessment by noninvasive in vivo diffusion tensor magnetic resonance imaging. J Neurosci Res 2006; 83: 392–402.

Helmstaedter C, Fritz NE, Gonzalez Perez PA, Elger CE, Weber B. Shift-back of right into left hemisphere language dominance after control of epileptic seizures: evidence for epilepsy driven functional cerebral organization. Epilepsy Res 2006; 70: 257–62.

Hoeft F, Barnea-Goraly N, Haas BW, Golarai G, Ng D, Mills D, et al. More is not always better: increased fractional anisotropy of superior longitudinal fasciculus associated with poor visuospatial abilities in Williams syndrome. J Neurosci 2007; 27: 11960–5.

Hugg JW, Kuzniecky RI, Gilliam FG, Morawetz RB, Fraught RE, Hetherington HP. Normalization of contralateral metabolic function following temporal lobectomy demonstrated by 1H magnetic resonance spectroscopic imaging. Ann Neurol 1996; 40: 236–9.

Hui ES, Fu QL, So KF, Wu EX. Diffusion tensor MR study of optic nerve degeneration in glaucoma. Conf Proc IEEE Eng Med Biol Soc 2007; 2007: 4312–5.

Jackson GD, Duncan JS. MRI atlas of the brain. New York: Churchill Livingstone; 1996.

Jain N, Florence SL, Qi HX, Kaas JH. Growth of new brainstem connections in adult monkeys with massive sensory loss. Proc Natl Acad Sci USA 2000; 97: 5546–50.

Jenkinson M, Bannister P, Brady M, Smith S. Improved optimization for the robust and accurate linear registration and motion correction of brain images. Neuroimage 2002; 17: 825–41.

Jenkinson M, Smith S. A global optimisation method for robust affine registration of brain images. Med Image Anal 2001; 5: 143–56.

Johansen-Berg H. Structural plasticity: rewiring the brain. Curr Biol 2007; 17: R141–4.

Jones DK, Symms MR, Cercignani M, Howard RJ. The effect of filter size on VBM analyses of DT-MRI data. Neuroimage 2005; 26: 546–54.

Joo EY, Hong SB, Han HJ, Tae WS, Kim JH, Han SJ, et al. Postoperative alteration of cerebral glucose metabolism in mesial temporal lobe epilepsy. Brain 2005; 128: 1802–10.

Kaas JH, Florence SL, Jain N. Subcortical contributions to massive cortical reorganizations. Neuron 1999; 22: 657–60.

Kinoshita Y, Ohnishi A, Kohshi K, Yokota A. Apparent diffusion coefficient on rat brain and nerves intoxicated with methylmercury. Environ Res 1999; 80: 348–54.

Leh SE, Johansen-Berg H, Ptito A. Unconscious vision: new insights into the neuronal correlate of blindsight using diffusion tractography. Brain 2006; 129: 1822–32.

Maccotta L, Buckner RL, Gilliam FG, Ojemann JG. Changing frontal contributions to memory before and after medial temporal lobectomy. Cereb Cortex 2007; 17: 443–56.

Makris N, Kennedy DN, McInerney S, Sorensen AG, Wang R, Caviness VS Jr, et al. Segmentation of subcomponents within the superior longitudinal fascicle in humans: a quantitative, in vivo, DT-MRI study. Cereb Cortex 2005; 15: 854–69.

Makris N, Pandya DN. The extreme capsule in humans and rethinking of the language circuitry. Brain Struct Funct 2009; 213: 343–58.

Makris N, Papadimitriou GM, Kaiser JR, Sorg S, Kennedy DN, Pandya DN. Delineation of the middle longitudinal fascicle in humans: a quantitative, in vivo, DT-MRI study. Cereb Cortex 2009; 19: 777–85.

May A, Gaser C. Magnetic resonance-based morphometry: a window into structural plasticity of the brain. Curr Opin Neurol 2006; 19: 407–11.

McKenna P, Warrington EK. Graded naming test manual. London: NFER Nelson; 1983.

Moran NF, Lemieux L, Maudgil D, Kitchen ND, Fish DR, Shorvon SD. Analysis of temporal lobe resections in MR images. Epilepsia 1999; 40: 1077–84.

Mori S, van Zijl PC. Fiber tracking: principles and strategies- a technical review. NMR Biomed 2002; 15: 468–80.

Mori S, Wakana S, Nagae-Poetscher LM, van Zijl PCM. MRI atlas of human white matter. Oxford: Elsevier; 2005.

Nichols TE, Holmes AP. Nonparametric permutation tests for functional neuroimaging: a primer with examples. Hum Brain Mapp 2002; 15: 1–25.

Noppeney U, Price CJ, Duncan JS, Koepp MJ. Reading skills after left anterior temporal lobe resection: an fMRI study. Brain 2005; 128: 1377–85.

Oldfield RC. The assessment and analysis of handedness: the Edinburgh inventory. Neuropsychologia 1971; 9: 97–113.

Pataraia E, Billingsley-Marshall RL, Castillo EM, Breier JI, Simos PG, Sarkari S, et al. Organization of receptive language-specific cortex before and after left temporal lobectomy. Neurology 2005; 64: 481–7.

Petrides M, Pandya DN. Association fiber pathways to the frontal cortex from the superior temporal region in the rhesus monkey. J Comp Neurol 1988; 273: 52–66.

Petrides M, Pandya DN. Efferent association pathways from the rostral prefrontal cortex in the macaque monkey. J Neurosci 2007; 27: 11573–86.

Petrides M, Pandya DN. Efferent association pathways originating in the caudal prefrontal cortex in the macaque monkey. J Comp Neurol 2006; 498: 227–51.

Petrides M, Pandya DN. Projections to the frontal cortex from the posterior parietal region in the rhesus monkey. J Comp Neurol 1984; 228: 105–16.

Pierpaoli C, Basser PJ. Toward a quantitative assessment of diffusion anisotropy. Magn Reson Med 1996; 36: 893–906.

Powell HW, Parker GJ, Alexander DC, Symms MR, Boulby PA, Wheeler-Kingshott CA, et al. Hemispheric asymmetries in language-related pathways: a combined functional MRI and tractography study. Neuroimage 2006; 32: 388–99.

Ramu J, Herrera J, Grill R, Bockhorst T, Narayana P. Brain fiber tract plasticity in experimental spinal cord injury: diffusion tensor imaging. Exp Neurol 2008; 212: 100–7.

Rueckert D, Sonoda LI, Hayes C, Hill DL, Leach MO, Hawkes DJ. Nonrigid registration using free-form deformations: application to breast MR images. IEEE Trans Med Imaging 1999; 18: 712–21.

Saur D, Kreher BW, Schnell S, Kummerer D, Kellmeyer P, Vry MS, et al. Ventral and dorsal pathways for language. Proc Natl Acad Sci USA 2008; 105: 18035–40.

Saur D, Lange R, Baumgaertner A, Schraknepper V, Willmes K, Rijntjes M, et al. Dynamics of language reorganization after stroke. Brain 2006; 129: 1371–84.

Schmahmann JD, Pandya DN. Disconnection syndromes of basal ganglia, thalamus, and cerebrocerebellar systems. Cortex 2008; 44: 1037–66.

Schmahmann JD, Pandya DN. Fibre pathways of the brain. New York: Oxford University Press; 2006.

Schmahmann JD, Pandya DN, Wang R, Dai G, D'Arceuil HE, de Crespigny AJ, et al. Association fibre pathways of the brain: parallel observations from diffusion spectrum imaging and autoradiography. Brain 2007; 130: 630–53.

Schoene-Bake JC, Faber J, Trautner P, Kaaden S, Tittgemeyer M, Elger CE, et al. Widespread affections of large fiber tracts in postoperative temporal lobe epilepsy. Neuroimage 2009; 46: 569–76.

Semah F, Picot MC, Adam C, Broglin D, Arzimanoglou A, Bazin B, et al. Is the underlying cause of epilepsy a major prognostic factor for recurrence? Neurology 1998; 51: 1256–62.

Smith SM, Jenkinson M, Johansen-Berg H, Rueckert D, Nichols TE, Mackay CE, et al. Tract-based spatial statistics: voxelwise analysis of multi-subject diffusion data. Neuroimage 2006; 31: 1487–505.

Smith SM, Jenkinson M, Woolrich MW, Beckmann CF, Behrens TE, Johansen-Berg H, et al. Advances in functional and structural MR image analysis and implementation as FSL. Neuroimage 2004; 23 (Suppl 1): S208–19.

Smith SM, Nichols TE. Threshold-free cluster enhancement: addressing problems of smoothing, threshold dependence and localisation in cluster inference. Neuroimage 2009; 44: 83–98.

Song SK, Sun SW, Ramsbottom MJ, Chang C, Russell J, Cross AH. Dysmyelination revealed through MRI as increased radial (but unchanged axial) diffusion of water. Neuroimage 2002; 17: 1429–36.

Spanaki MV, Kopylev L, DeCarli C, Gaillard WD, Liow K, Fazilat S, et al. Postoperative changes in cerebral metabolism in temporal lobe epilepsy. Arch Neurol 2000; 57: 1447–52.

Spreen O, Strauss E. A compendium of neuropsychological tests. New York: Oxford University Press; 1998.

Sun SW, Liang HF, Cross AH, Song SK. Evolving Wallerian degeneration after transient retinal ischemia in mice characterized by diffusion tensor imaging. Neuroimage 2008; 40: 1–10.

Vollmar C, O'Muircheartaigh J, Barker GJ, Symms MR, Thompson P, Kumari V, et al. Identical, but not the same: intra-site and inter-site reproducibility of fractional anisotropy measures on two 3.0T scanners. Neuroimage 2010; 51: 1384–94.

Wiebe S, Blume WT, Girvin JP, Eliasziw M. A randomized, controlled trial of surgery for temporal-lobe epilepsy. N Engl J Med 2001; 345: 311–8.

Wieser HG, Blume WT, Fish D, Goldensohn E, Hufnagel A, King D, et al. ILAE Commission Report. Proposal for a new classification of outcome with respect to epileptic seizures following epilepsy surgery. Epilepsia 2001; 42: 282–6.

Wilke M, Lidzba K. LI-tool: a new toolbox to assess lateralization in functional MR-data. J Neurosci Methods 2007; 163: 128–36.

Woermann FG, Barker GJ, Birnie KD, Meencke HJ, Duncan JS. Regional changes in hippocampal T2 relaxation and volume: a quantitative magnetic resonance imaging study of hippocampal sclerosis. J Neurol Neurosurg Psychiatry 1998; 65: 656–64.

Wong SW, Jong L, Bandur D, Bihari F, Yen YF, Takahashi AM, et al. Cortical reorganization following anterior temporal lobectomy in patients with temporal lobe epilepsy. Neurology 2009; 73: 518–25.

Wu Q, Butzkueven H, Gresle M, Kirchhoff F, Friedhuber A, Yang Q, et al. MR diffusion changes correlate with ultra-structurally defined axonal degeneration in murine optic nerve. Neuroimage 2007; 37: 1138–47.

Yasuda CL, Valise C, Saude AV, Pereira AR, Pereira FR, Ferreira Costa AL, et al. Dynamic changes in white and gray matter volume are associated with outcome of surgical treatment in temporal lobe epilepsy. Neuroimage 2009; 49: 71–9.